

cooling and other diffusional operations. It has been studied extensively and their references can be found in the books by Schlichting [1], Eckert [2] and Rosenhead [3] etc. These studies have employed the classical boundary-layer equations and hence are valid for very high value of Reynolds number. At moderately large Reynolds number, however, it is well-known that the boundary-layer equations require certain higher order corrections (Van Dyke [4]), attributed to arise from (i) longitudinal curvature, (ii) transverse curvature, (iii) displacement speed, (iv) external vorticity and (v) temperature gradient in the on-coming stream.

For an impermeable wall ($v_w = 0$) the general structure of self-similarity for second-order effects has been studied by Afzal and Oberai [5] and Werle and Davis [6]. Afzal and Raisinghani [7] have studied the heat transfer problem for full similarity with viscous dissipation.

It is the purpose of the present work to study the effect of suction and injection on self-similar solutions of second-order momentum and energy-equations with full similarity in viscous dissipation terms. In the framework of second-order theory a general expression for normal velocity v_w ($v_w < 0$ for suction and $v_w > 0$ for injection) is taken as

$$v_w = R^{-\frac{1}{2}}v_{w1} + R^{-1}v_{w2} + \dots, \tag{1}$$

where v_{w1} is the first-order normal velocity and v_{w2} the second-order normal velocity at the surface. As the second-order boundary-layer equations are linear, hence in addition to the above mentioned five effects one more effect due to v_{w2} has been separated.

Earlier Wannous and Sparrow [8] have analysed the transverse curvature effect with suction and injection by studying momentum transfer for axisymmetric flow along a circular cylinder. In the variables of present work their study correspond to $\Lambda_r = 0, \beta = 0$.

2. FORMULATION

The Navier-Stokes and the energy equation in usual non-dimensional notations are

$$\text{div } \mathbf{U} = 0, \tag{2}$$

$$\mathbf{U} \cdot \text{grad } \mathbf{U} + \text{grad } P = -R^{-1} \text{curl curl } \mathbf{U}, \tag{3}$$

$$\mathbf{U} \cdot \text{grad } T - \sigma^{-1} R^{-1} \nabla^2 T = R^{-1} \text{grad } \mathbf{U} \cdot \text{def } \mathbf{U}. \tag{4}$$

Where R is the characteristic Reynolds number, σ the Prandtl number. The boundary conditions at the surface are

$$U = 0, \quad V = v_w(s) \tag{5a, b}$$

$$T = t_w(s) \quad \text{or} \quad \text{grad } T = 0. \tag{5c}$$

Where $v_w(s)$ is given by equation (1). Far upstream the flow has to approach prescribed, may be non-uniform velocity and temperature fields.

The second-order boundary-layer equations are obtained from Navier-Stokes equations by the method of matched asymptotic expansions [4, 7]. In this method two limits are defined: an outer limit (defined as n fixed, $R \rightarrow \infty$) and the inner limit ($N = nR^{\frac{1}{2}}$ fixed,

$R \rightarrow \infty$). The corresponding two expansions for a typical variable are given below

$$\text{Outer expansion: } \phi = \Phi_1 + R^{-\frac{1}{2}}\Phi_2 + \dots \tag{6a}$$

$$\text{Inner expansion: } \phi = \phi_1 + R^{-\frac{1}{2}}\phi_2 + \dots \tag{6b}$$

Thus first and second-order boundary-layer equations obtained through matching are as follows.

First-order boundary-layer equations:

$$\begin{aligned} (r^j u_1)_s + (r^j v_1)_N &= 0, \\ u_1 u_{1s} + v_1 u_{1N} - U_1(s, 0) U_{1s}(s, 0) - u_{1NN} &= 0, \\ u_1 t_{1N} + v_1 t_{1N} - \sigma^{-1} t_{1NN} - u_{1N}^2 &= 0, \\ u_1(s, 0) = 0, \quad v_1(s, 0) = v_{w1}(s), & \tag{7} \\ u_1(s, N) \sim U_1(s, 0) \quad \text{as } N \rightarrow \infty, & \\ t_1(s, 0) = t_w(s) \quad \text{or} \quad t_{1N}(s, 0) = 0, & \\ t_1(s, N) \sim H_1(0) \quad \text{as } N \rightarrow \infty. & \end{aligned}$$

Second-order boundary-layer equations:

$$\begin{aligned} (r^j u_2)_s + (r^j v_2)_N &= -[r^j(j \cos \theta/r)Nu_1]_s - [r^j(K + j \cos \theta/r)Nv_1]_N, \\ u_1 u_{2s} + u_2 u_{1s} + v_1 u_{2N} + v_2 u_{1N} - u_{2NN} &= K[Nu_1 u_{1s} - u_1 v_1 - NU_1(s, 0)U_{1s}(s, 0) + u_{1N}] \\ - \left[KN U_1^2(s, 0) + K \int_N^\infty U_1^2(s, 0) - u_1^2 dN \right]_s & \\ + u_{1N} j \cos \theta/r - r^j B_1'(0) V_2(s, 0) & \\ + [U_1(s, 0)U_2(s, 0)]_s, & \tag{8} \\ u_1 t_{2s} + u_2 t_{1s} + v_1 t_{2N} + v_2 t_{1N} - \sigma^{-1} t_{2NN} - 2u_{1N} u_{2N} & \\ = K(Nu_1 t_{1s} + \sigma^{-1} t_{1N} - 2u_1 u_{1N}) + \sigma^{-1} j \cos \theta t_{1N}/r, & \\ u_2(s, 0) = 0, \quad v_2(s, 0) = v_{w2}, & \\ u_2(s, N) \sim NKU_1(s, 0) + r^j NB_1'(0) + U_2(s, 0) & \\ \text{as } N \rightarrow \infty, & \\ t_2(s, 0) = 0 \quad \text{or} \quad t_{2N}(s, 0) = 0, & \\ t_2(s, N) \sim H_1'(0) = \left(\frac{\partial H_1}{\partial \Psi_1} \right)_{\Psi_1=0} \quad \text{as } N \rightarrow \infty. & \end{aligned}$$

In the following analysis all the capital letters $U_1(s, 0), H_1(s, 0), B_1(0)$ etc. will be used without their arguments, i.e. as U_1, H_1, B_1 etc.

3. SIMILARITY ANALYSIS

In the present analysis, Gortler's variables

$$\zeta = \int_0^s U_1 r^{2j} ds, \quad \eta = \frac{r^j N U_1}{\sqrt{(2\xi)}} \tag{9, 10}$$

have been used.

3.1. First-order problem

The well known form of the stream function which gives similarity for first-order momentum equation is

$$\psi_1(s, N) = (2\xi)^{\frac{1}{2}} f(\eta). \tag{11}$$

Using (9), (10) and (11), the momentum equation reduces to

$$f''' + ff'' + \beta(1 - f'^2) = 0, \tag{12}$$

$$f(0) = C, \quad f'(0) = 0, \quad f'(\infty) = 1. \tag{13a, b, c}$$

Here β is the Falkner-Skan pressure gradient and C ,

the first-order suction parameter are assumed constants. They are defined as

$$\beta = \frac{2\xi}{U_1} \frac{dU_1}{d\xi}, \quad C = -v_{w1}(2\xi)^{\frac{1}{2}}/(U_1 r^j). \quad (14, 15)$$

The equation (12) is the well known Falkner-Skan equation whose solutions with the boundary conditions (13) have been studied extensively [1, 2, 3].

For temperature profile, the similarity variable is

$$t_1(s, N) = (t_w - H_1)[g_1(\eta) + Eg_2(\eta)] + H_1. \quad (16)$$

In writing down the relation (16), the linearity of energy equation is exploited and as such the equations for the functions g_1 and g_2 are independent of

$$E [= U_1^2/(t_{w1} - H_1)]$$

The functions B_i 's are defined as

$$B_1 = \sqrt{(2\xi)K}/(r^j U_1), \quad B_t = \sqrt{(2\xi)j \cos \theta}/(r^{2j} U_1), \quad (23, 24)$$

$$B_d = U_2/U_1, \quad (25)$$

$$B_v = \sqrt{(2\xi)B_1/U_1^2}, \quad B_e = \sqrt{(2\xi)H_1/U_1^2}, \quad (26)$$

$$B_e = \sqrt{(2\xi)H_1'/(t_w - H_1)}, \quad (27)$$

$$B_w = -v_{w2} \sqrt{(2\xi)/(U_1 r^j)}. \quad (28)$$

Here B_1 arises due to longitudinal curvature, B_t due to transverse curvature, B_d due to displacement speed, B_v due to external vorticity, B_e due to temperature gradient and B_w due to normal velocity v_{w2} . Using (21) and (22), the second-order equations may be written

Table 1. Values of functions used in second-order equations (29-34)

	i	Λ_i	a_i	b_i	d_i	A_i	B_i	D_i
Longitudinal curvature	1	Λ_1	$-\eta f''' + [(\Lambda_1 + \beta - 1)(f'' + ff') + (2\beta + \Lambda_1)(\beta\eta + \delta)]/(1 + \beta)$	0	$-\eta$	$-\sigma^{-1}(\eta g_1)'$	0	$-\sigma^{-1}(\eta g_2)' + f''(-\eta f'' + 2f')$
Transverse curvature	t	Λ_t	$-\eta(2\beta + f''') + f'' + ff' - \Lambda_t \eta f'^2$	0	η	$-\sigma^{-1}(\eta g_1)'$	0	$-\sigma^{-1}(\eta g_2)' + f''(\eta f'' + 2f'')$
Displacement speed	d	Λ_d	$-2\beta - \Lambda_d$	0	1	0	0	0
External vorticity	v	$1 - 2\beta$	$-\delta$	0	η	0	0	0
Temperature gradient in on-coming stream	e	$1 - 2\beta$	0	0	0	0	$\eta - \delta$	0
Suction velocity v_{w2}	w	Λ_w	0	1	0	0	0	0

the Eckert number. For full similarity with viscous dissipation E has to be constant, which yields $\Lambda_{t_w-H_1} = 2\beta$. The governing equations for g_1 and g_2 take the form

$$\sigma^{-1}g_1'' + fg_1' - 2\beta f'g_1 = 0, \quad (17)$$

$$g_1(0) = 1, \quad g_1(\infty) = 0, \quad (18a, b)$$

$$\sigma^{-1}g_2'' + fg_2' - 2\beta f'g_2 + f''^2 = 0, \quad (19)$$

$$g_2(0) = 0 = g_2(\infty). \quad (20a, b)$$

3.2. Second-order problem

The second-order boundary-layer equations are linear and hence can be divided into a number of simpler problems. For flows over an impermeable surface, it has been divided into the five effects, mentioned earlier. When velocity $v_{w2} \neq 0$, an additional sixth effect due to v_{w2} can also be linearly separated. For the six effects the second-order stream function ψ_2 and temperature t_2 are assumed as

$$\psi_2 = \sqrt{(2\xi)} \sum_i B_i F^{(i)}(\eta) \quad (21)$$

$$t_2 = (t_w - H_1) \sum B_i [G_1^{(i)}(\eta) + EG_2^{(i)}(\eta)] \quad (22)$$

where $i = 1, t, d, v, e, w$.

in the operator form as

$$F^{(i)'''} + fF^{(i)''} - (2\beta + \Lambda_i)f'F^{(i)'} + (1 + \Lambda_i)f''F^{(i)} = a_i, \quad (29)$$

$$F^{(i)}(0) = b_i, \quad F^{(i)}(\infty) = 0,$$

$$F^{(i)}(\eta) \sim d_i \quad \text{as } \eta \rightarrow \infty, \quad (30)$$

$$\sigma^{-1}G_1^{(i)''} + fG_1^{(i)'} - (2\beta + \Lambda_i)f'G_1^{(i)} + (1 + \Lambda_i)F^{(i)}g_1' - 2\beta F^{(i)'}g_1 = A_i, \quad (31)$$

$$G_1^{(i)}(0) = 0, \quad G_1^{(i)}(\eta) \sim B_i \quad \text{as } \eta \rightarrow \infty. \quad (32)$$

$$\sigma^{-1}G_2^{(i)''} + fG_2^{(i)'} - (2\beta + \Lambda_i)f'G_2^{(i)} + (1 + \Lambda_i)F^{(i)}g_2' - 2\beta F^{(i)'}g_2 + 2f''F^{(i)} = D_i, \quad (33)$$

$$G_2^{(i)}(0) = 0 = G_2^{(i)}(\infty), \quad (34)$$

where subscript i takes the values 1, t , d , v , e and w . For various second-order problems the functions Λ_i , a_i , b_i , d_i , A_i , B_i and D_i are given in Table 1. Here Λ_i is defined by the equation

$$\Lambda_i = (2\xi/B_i)(\partial B_i/\partial \xi) \quad i = 1, t, d, v, w, e \quad (35)$$

and has to be constant for self similar solutions.

The skin friction τ in nondimensional form is

$$\tau = r^j U_1^2 (2R\xi)^{-\frac{1}{2}} [f''(0) + R^{-\frac{1}{2}} \sum_i B_i F_i^{(j)'}(0) + \dots], \quad (36)$$

and the displacement thickness is

$$\Delta = R^{-\frac{1}{2}} \sqrt{(2\xi)/(r^j U_1)} \delta + R^{-1} \left[\sqrt{(2\xi) U_2 / (r^j U_1^2)} \delta^{(d)} + 2\xi / (r^{2j} U_1^2) \times \{r^j B_1 / U_1 \delta^{(v)} + K \delta^{(l)} + j \cos \theta / r \delta^{(t)} - \delta^{(w)} v_{w2} / \sqrt{(2\xi)}\} \right]. \quad (37)$$

Where

$$\left. \begin{aligned} \delta &= \eta - f \\ \delta^{(1)} &= -\frac{1}{2} \eta^2 - F^{(1)} + \frac{1}{2} \delta^2 \\ \delta^{(t)} &= \frac{1}{2} \eta^2 - F^{(t)} - \frac{1}{2} \delta^2 \\ \delta^{(d)} &= \eta - F^{(d)} - \delta \\ \delta^{(v)} &= \frac{1}{2} \eta^2 - F^{(v)} - \frac{1}{2} \delta^2 \\ \delta^{(w)} &= 1 - F^{(w)} \end{aligned} \right\} \text{ as } \eta \rightarrow \infty. \quad (38)$$

The expression for heat transfer is given by

$$q = \sigma^{-1} r^j U_1 (2\xi)^{-\frac{1}{2}} R^{-\frac{1}{2}} \times [g_1'(0) + E g_2'(0) + R^{-\frac{1}{2}} \sum_i B_i \{G_1^{(i)'}(0) + E G_2^{(i)'}(0)\} + \dots]. \quad (39)$$

The recovery temperature t_r is defined as temperature of the wall for which there is no heat transfer at the surface. It is generally expressed in terms of dimensionless recovery factor r_f , defined as

$$r_f = 2(t_r - H_1) / U_1^2 = r_1 + R^{-\frac{1}{2}} r_2 + \dots \quad (40)$$

where r_1 and r_2 are first-order and second-order recovery factors, given by

$$\begin{aligned} r_1 &= -2g_2'(0) / g_1'(0), & r_2 &= \sum_i B_i r_2^{(i)}, & (41, 42) \\ i &= 1, t, d, v, w, \bar{e} \\ r_2^{(t)} &= 2[g_2'(0)G_1^{(t)}(0) - g_1'(0)G_2^{(t)}(0)] / g_1'^2(0), \\ i &= 1, t, d, v, w, \\ r_2^{(v)} &= 2G_1^{(v)'} / g_1'(0). \end{aligned}$$

The expression for heat transfer (44) for full similarity with viscous dissipation can further be simplified in terms of t_r as

$$q = -\sigma^{-1} r^j U_1 (t_w - t_r) (2\xi R)^{-\frac{1}{2}} \times [g_1'(0) + R^{-\frac{1}{2}} \sum_i B_i G_i^{(j)'}(0) + \dots], \quad i = 1, t, d, v, w.$$

This shows that the heat transfer is zero when $t_w = t_r$.

4. RESULTS AND DISCUSSION

The first and second-order boundary-layer equations are two point boundary value problems and have been integrated numerically by Runge-Kutta-Gill method on IBM 7044 computer. In order to limit the truncation error, a conservative value of step size $\Delta\eta = 0.05$ was selected (Smith [10]). The first-order momentum equation is non-linear, its solutions accurate to five places of decimals were obtained by using the values of Stewart and Probe [11] as the initial guess values.

These results were successively employed to integrate the second-order linear equations and the results are believed to be correct to five decimal places. The present results compare well with the available no suction results of [7]. The equations have been solved for various values of suction parameter C in the range of $-0.6 \leq C \leq 0.6$. The ranges for other parameters are $-7.5 \leq \Lambda_1, \Lambda_r, \Lambda_d, \Lambda_w \leq 4, \beta = 0, 0.5$ and 1 and $\sigma = 0.7, 3$ and 5 . Results for second-order contributions to skin-friction $F''(0)$, heat transfer $G_1'(0)$ and recovery factor r_2 are displayed graphically. The results for $G_2'(0)$ can be obtained from those for $G_1'(0)$ and r_2 .

Figure 2(a) shows skin-friction $F''(0)$ vs Λ_1 for $\beta = 0.5$ and two fixed values of suction parameter $C = 0.5$ and -0.5 . For $\Lambda_1 < 0$, we observe many singularities. The location of first singularity for $C = 0$ (no suction or injection) is also shown in the same graph by a vertical arrow which is at $\Lambda_1 = -3.1$ (Afzal and Oberai [5]). For $C = 0.5$ (suction) this singularity occurs at $\Lambda_1 = -3.5$ and for $C = -0.5$ (injection) at $\Lambda_1 = -2.72$. The effect of suction (injection) on the location of singularity is to increase (decrease) the value of negative Λ_1 . It may be noted that the effect of suction is qualitatively the same as that of favourable pressure gradient, i.e. for a given suction if β increases the value of Λ_1 increase in magnitude. Figures 2(b) and 2(c) show the effects of a given suction or injection on heat transfer

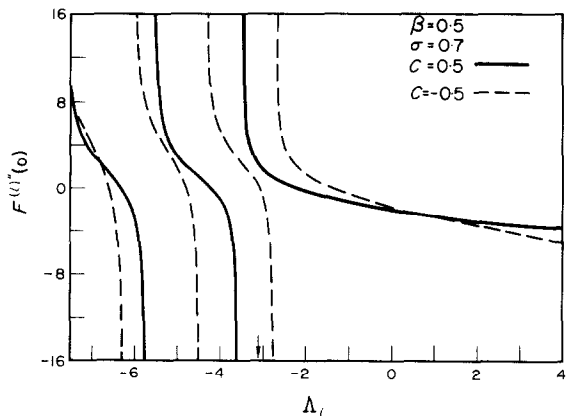


FIG. 2(a). Longitudinal curvature solutions: effects of suction and injection on locations of singularities in skin friction.

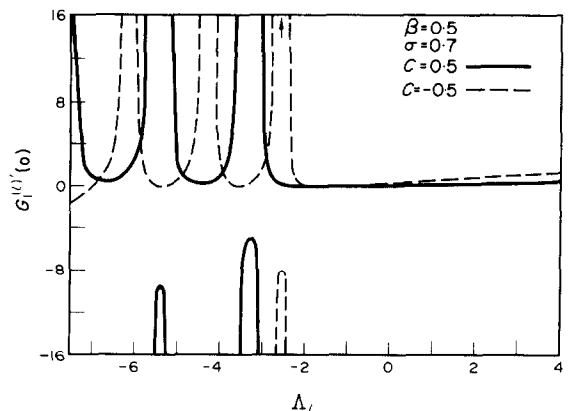


FIG. 2(b). Longitudinal curvature solutions: effects of suction and injection on location of singularities in heat transfer.

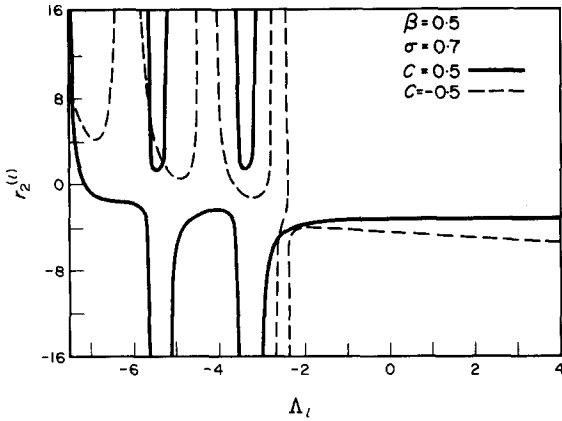


FIG. 2(c). Longitudinal curvature solutions: effects of suction and injection on locations of singularities on recovery factor.

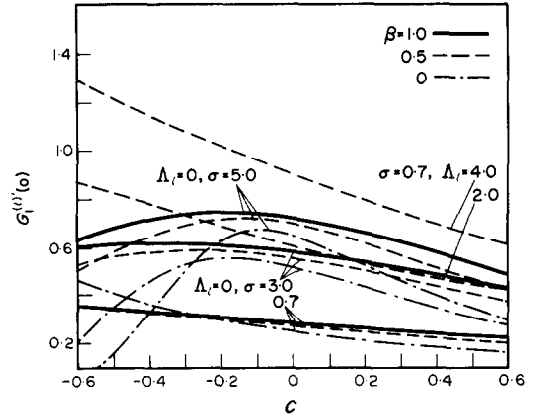


FIG. 3(b). Longitudinal curvature solutions: effects of suction and injection on heat transfer.

$G_1'(0)$ and recovery factor r_2 respectively. Here the approximate location of first singularity for $C = 0$ is at $\Lambda_1 = -2.75$, (shown by arrow) for $C = 0.5$ at $\Lambda_1 = -3.0$ and for $C = -0.5$ at $\Lambda_1 = -2.32$. It is to be observed that for a fixed value of suction parameter C , the singularity in $G_1'(0)$ and r_2 occurs at lower values of negative Λ_1 when compared to the corresponding skin friction, results. This is due to the fact that the critical value (eigenvalue) for the homogeneous energy problem is lower than the corresponding momentum problem. For transverse curvature, displacement speed problems, the effect of suction and injection on the location of singularities is similar to those described as above and may be referred to [9].

The effect of suction parameter C for longitudinal curvature, transverse curvature, displacement speed, external vorticity and temperature gradient problems on skin friction $F''(0)$, displacement thickness, heat transfer $G_1'(0)$ and recovery factor r_2 are shown in Figs. 3(a-c) to Figs. 7(a-b). From these figures, it is observed that the relative variation of second-order heat transfer with suction parameter C decreases as β increases for a given value of σ .

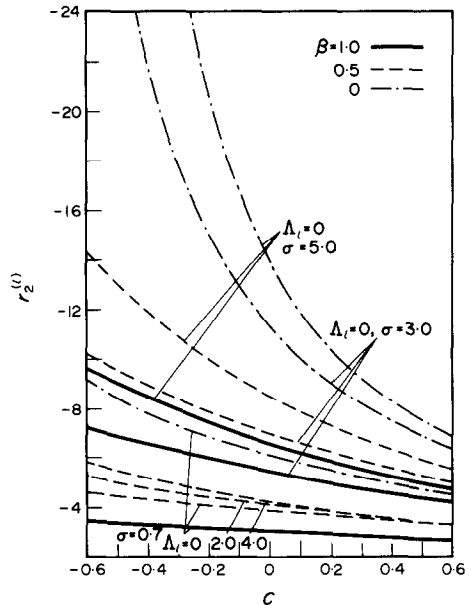


FIG. 3(c). Longitudinal curvature solutions: effects of suction and injection on recovery factor.

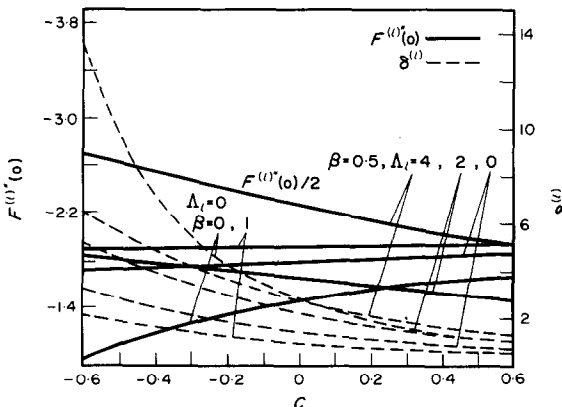


FIG. 3(a). Longitudinal curvature solutions: effects of suction and injection on skin friction and displacement thickness.

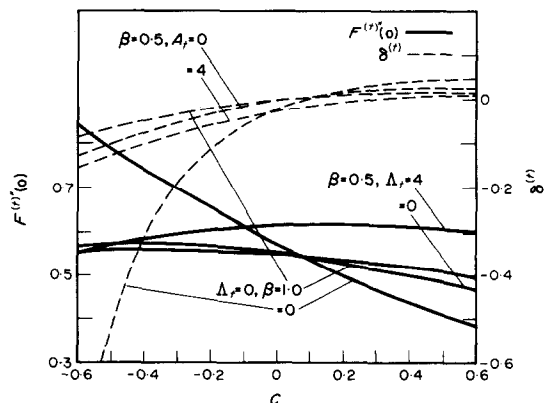


FIG. 4(a). Transverse curvature solutions: effects of suction and injection on skin friction and displacement thickness.

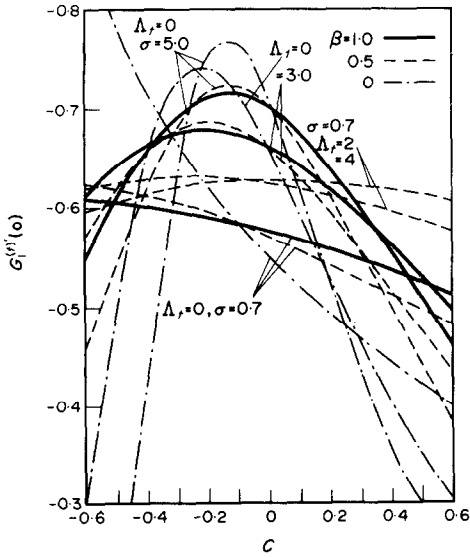


FIG. 4(b). Transverse curvature solutions: effects of suction and injection on heat transfer.

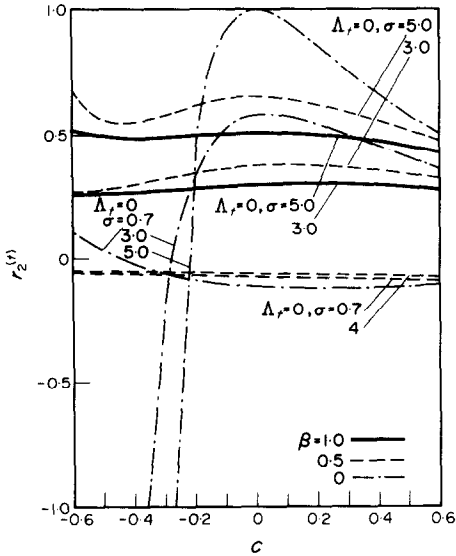


FIG. 4(c). Transverse curvature solutions: effects of suction and injection on recovery factor.

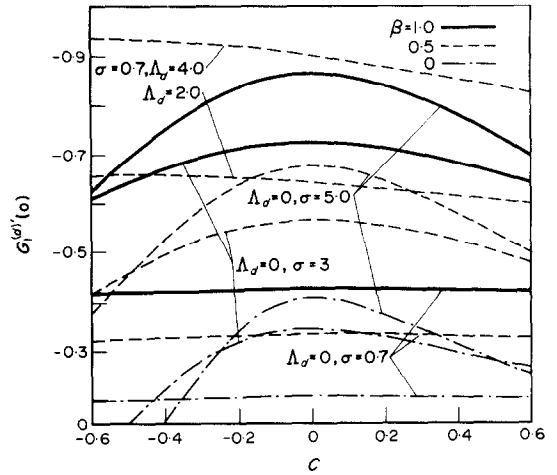


FIG. 5(b). Displacement speed solutions: effects of suction and injection on heat transfer.

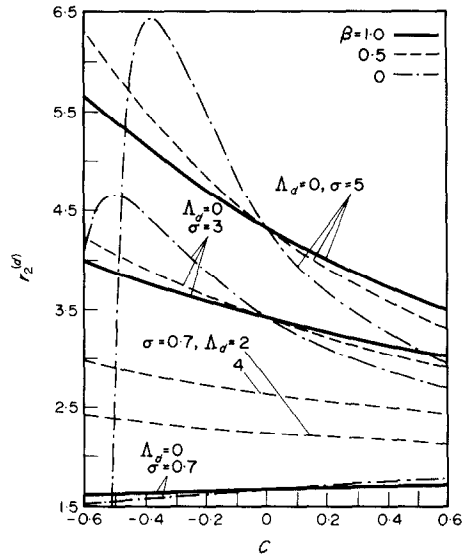


FIG. 5(c). Displacement speed solutions: effects of suction and injection on recovery factor.

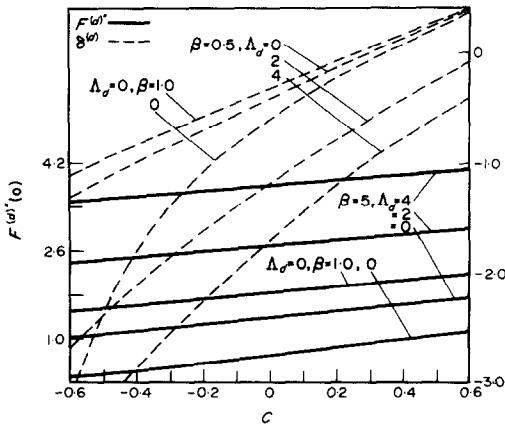


FIG. 5(a). Displacement speed solutions: effects of suction and injection on skin friction and displacement thickness.

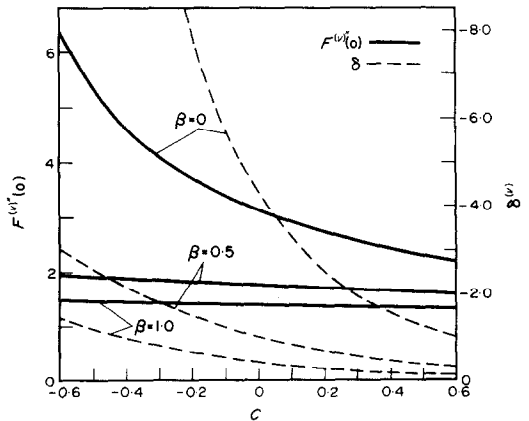


FIG. 6(a). External vorticity solutions: effects of suction and injection on skin friction and displacement thickness.

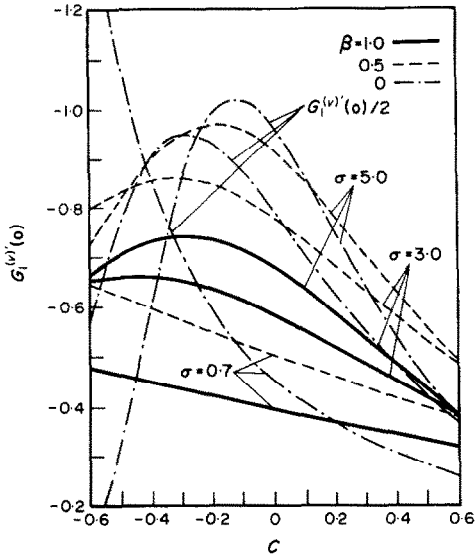


FIG. 6(b). External vorticity solutions: effects of suction and injection on heat transfer.

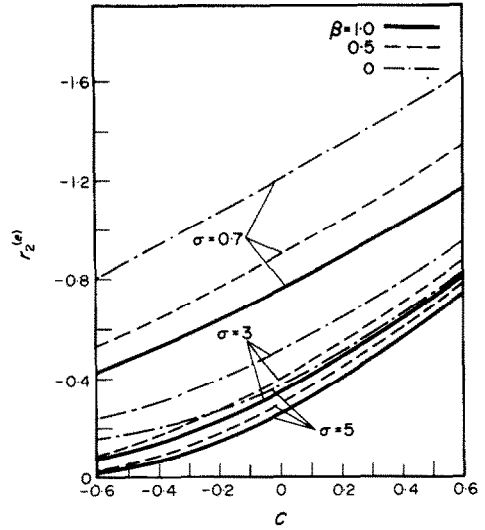


FIG. 7(b). Temperature gradient solutions: effects of suction and injection on recovery factor.

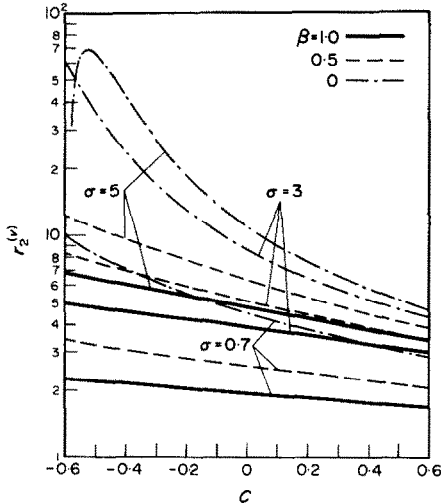


FIG. 6(c). External vorticity solutions: effects of suction and injection on recovery factor.

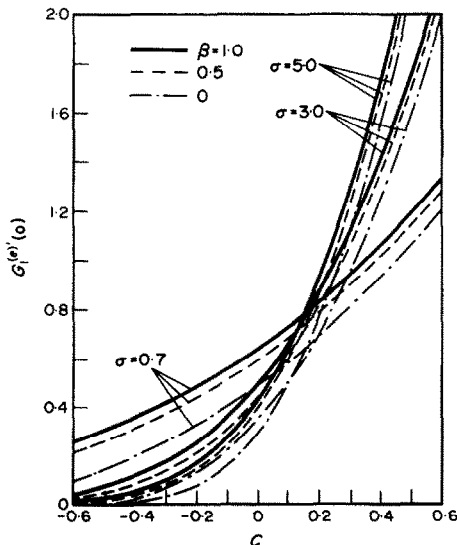


FIG. 7(a). Temperature gradient solutions: effects of suction and injection on heat transfer.

We now consider the second-order effect due to v_{w2} shown in Figs. 8(a-c). The suction velocity v_w has both first and second-order components v_{w1} and v_{w2} . In order to distinguish between the two components, we first describe the effect due to v_{w2} when the first-order suction velocity v_{w1} (or C) is zero, i.e. $v_w \sim O(R^{-1})$. Figure 8(a) shows the second-order effect due to v_{w2} on skin friction and displacement thickness plotted against the parameter C . For $C = 0$, $\Lambda_w \geq 0$, it is observed that second-order contribution to skin friction increases as β decreases. As the first and second-order contributions are of the same sign, the second-order suction increases the total skin friction. This trend is qualitatively similar to classically well-known first-order suction effect. However for $\Lambda_w < 0$ no such statement can be made due to the presence of singularities mentioned earlier. The effect of first-order suction parameter C will now be described on second-order contribution. As C increases, the second-order contribution to skin friction for any fixed value of β and

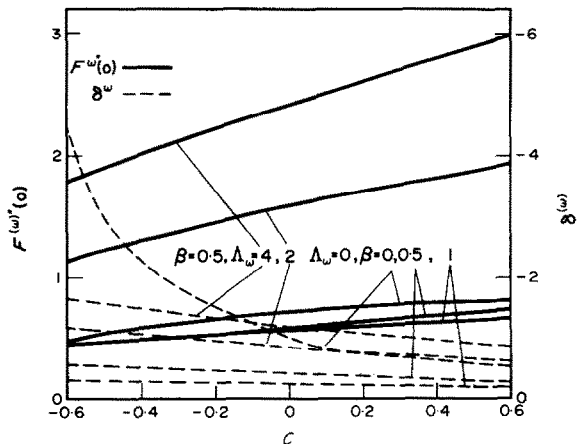


FIG. 8(a). Solutions for second-order suction effect: skin friction and displacement thickness.

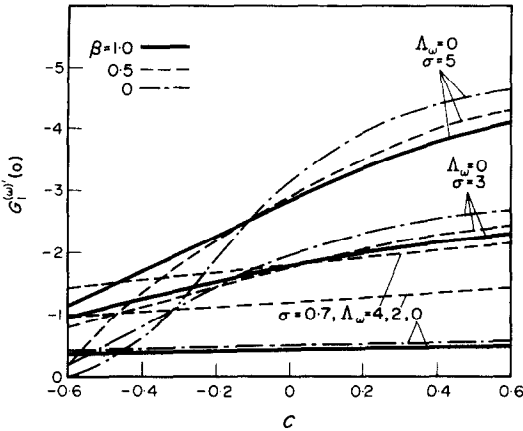


FIG. 8(b). Solutions for second-order suction effect: heat transfer.

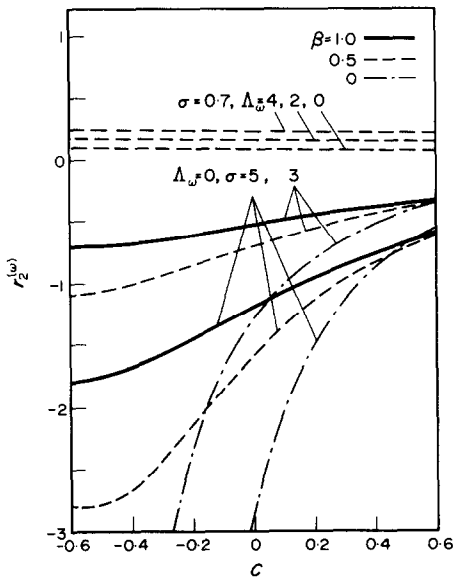


FIG. 8(c). Solutions for second-order suction effect: recovery factor.

Λ_w also increases. The rate of increase becomes more pronounced as Λ_w increases for a given value of β ($=0.5$).

Figures 8(b) and 8(c) show second-order contributions to heat transfer and recovery-factor respectively. For the case $v_w \sim O(R^{-1})$, we note that the second-order contribution to heat transfer (recovery factor) increases in magnitude as β increases (decreases)

for $\Lambda_w \geq 0$. The interaction of first-order and second-order suction shows that the second-order contribution to heat transfer and recovery-factor increases in magnitude as C increases. The rate of increase becomes more and more pronounced for decreasing values of β and increasing values of σ .

REFERENCES

1. H. Schlichting, *Boundary-Layer Theory*, 6th edn. McGraw-Hill, New York (1968).
2. E. R. C. Eckert, *Analysis of Heat and Mass Transfer*, McGraw-Hill, New York (1972).
3. L. Rosenhead, *Laminar Boundary-Layers*. Clarendon Press, Oxford (1963).
4. M. Van Dyke, Higher approximations in boundary-layer theory. Part I: General analysis, *J. Fluid Mech.* **14**, 161-177 (1962).
5. N. Afzal and M. M. Oberai, Self-similar solutions of the second-order boundary-layer of an incompressible fluid with heat transfer. *Int. J. Heat Mass Transfer* **15**, 99-113 (1972).
6. M. J. Werle and R. T. Davis, Self-similar solutions to the second-order incompressible boundary-layer equations, *J. Fluid Mech.* **40**, 343-360 (1970).
7. N. Afzal and S. C. Raisinghani, Heat transfer due to second-order boundary-layer flows with dissipation, *J. Aeronaut. Soc., India* **25**, 56-66 (1973).
8. D. J. Wannous and E. M. Sparrow, Longitudinal flow over a circular cylinder with surface mass transfer, *AIAA JI* **3**, 147-148 (1965).
9. Shabbir Ahmad, Effect of suction and injection on self-similar solutions of second-order boundary-layer equations, M. Tech. Thesis, I.I.T. Kanpur (1973).
10. A. M. O. Smith, Improved solutions of the Falkner and Skan boundary-layer equations, Inst. of Aero. Sci. S.M.F. Fund Paper No. FF 10 (1954).
11. W. E. Stewart and R. Prober, Heat transfer and diffusion in wedge flows with rapid mass transfer. *Int. J. Heat Mass Transfer* **5**, 1149-1163 (1962).

NOTE ADDED IN PROOF

Alternatively, instead of equations (21) and (22), the second-order effects can also be separated in such a way that a part of displacement effect is included in the suction effect, i.e.

$$\Psi_2 = (2\zeta)^{\frac{1}{2}} [B_1 F^{(1)}(\eta) + B_1 F^{(1)}(\eta) + B_d F_*^{(d)}(\eta) + (B_w - B_d C/2) F_*^{(w)}(\eta)]$$

along with a similar expression for t_2 . This has the advantage that for a special case $\Lambda_d = \Lambda_w = 0$, the displacement equations for $F_*^{(d)}$ etc. admit the following closed form solutions:

$$\begin{aligned} F_*^{(d)} &= (\eta f' + f)/2 \\ G_{*1}^{(d)} &= \eta g'_1/2 \\ G_{*2}^{(d)} &= 2g_2 + \eta g'_2/2. \end{aligned}$$

Further, the equations for $F_*^{(w)}$ etc. still satisfy the equations identical to those of $F^{(w)}$ etc.